TECHNICAL NOTE

ON THE ELASTIC STABILITY OF SLEEVE STIFFENED HOLLOW COLUMNS; FOCUSING ON DETERMINATION OF OPTIMAL DESIGN CURVES

A. Sinaie and H. Shahi

School of Engineering
Shahid Bahonar University of Kerman

Abstract The stability analysis of sleeve stiffened pin-ended slender hollow columns of pipe or box sections is performed in the present study. This is accomplished by using energy method, employing three terms in the assumed approximate deflection function. The lengthy and tedious algebraic manipulations involved in solving the relevant eigenvalue problem, necessitates employing the "MATHEMATICA" software. Nevertheless, the final result for the critical load can not be presented in a closed from equation, as it is too long and may occupy several pages. The critical loads are determined for many different box and pipe sizes. A total of 144 design curves are determined and plotted showing the critical load for different lengths and thicknesses of the stiffening sleeve. The curves show an increasing trend in buckling load-carrying capacity up to 90 percent. Minimizing the material volume of the sleeves, the optimal portions of the design curves are determined. It is also found that sleeve stiffening beyond 70 percent of the length of the column is a waste of material, as it does not significantly contribute to increasing the load carrying capacity. The possibility of local shell buckling is also considered.

Key Words Elastic Stability, Buckling, Stiffened Columns, Design Curves

چکیده در این مقاله، پایداری ستونهای توخالی با تقویت غلافی، مورد بررسی قرار گرفته است. ستونها می توانند دارای مقطع قوطی یا لوله بوده و دو سر مفصل فرض می شوند. با استفاده از روش انرژی، با در نظر گرفتن سه عبارت در منحنی تغییر شکل فرضی، بار بحرانی برای ستونهای تقویت شده بر حسب طول و ضخامت عضو تقویتی تعیین شده و با استفاده از روابط بدست آمده، تعداد ۱۴۴ منحنی طرح برای ابعاد مختلف مقاطع تهیه شده است. منحنی های طرح تا ۹۰٪ افزایش باربری را نشان می دهند. همچنین منحنی ها نشان می دهند که افزایش طول تقویت بیش از ۰/۷ طول ستون، تاثیر چندانی در افزایش ظرفیت باربری ندارد. با حداقل نمودن حجم ماده مصرفی، بخشهای بهینه منحنی های طرح نیز تعیین شده اند. برای ستونهایی که نمی توانند بلند و لاغر تلقی شوند، کمانش موضعی (پوسته ای) نیز بررسی شده است. به علت طولانی بودن بیش از حد روابط و محاسبات، کلیه عملیات ریاضی با استفاده از نرم افزار «متمتیکا» انجام پذیرفته است.

INTRODUCTION

The selection of structural and machine elements is based on three characteristics; strength, stiffness, and stability. The pioneer works of Euler [1] on the stability of compression members dates back to as early as 1744. Euler's work was considered doubtful until Shanley [2,3] in 1946 presented an explanation of the behavior of columns under compressive forces. Hoff [4] and Johnston [5] have reviewed the progress of stability analysis in different periods of time. Recent investigations involve a wide range of problems like post buckling of columns, composite cylindrical shell, and variable-thickness columns, among others,. Koiter et. al. [6] focused on the buckling of cylindrical shells with small thickness variations. Asymptotic formulas up to the second order of the thickness were derived by the combination of perturbation method and weighted residual method. Results were compared to numerical technique of finite difference. Ross and Humphries [7] tested several partially corrugated circular cylinders to destruction and observed that some of the cylinders failed by inelastic general instability and some by local buckling mode. They concluded that neither the classical shell instability mode prevailed nor the classical general instability mode. This behavior was attributed to the out of roundness initially presented in the cylinders. Barbero and Tombling [8] investigated Euler buckling of thin walled composite columns and also experimentally determined the critical loads. The results were compared and reported to show a reasonably good agreement with these of theoretical predictions. Wang et. al. [9] researched on elastic buckling of columns to find approximate formulas and also design charts. In their work, they sacrificed accuracy for the sake of simplicity. Development of a user friendly powerful software for the design of columns, beams and plates to withstand buckling was suggested by them. Lin et.al. [10] derived energy equatons for lateral buckling and concluded that theoretical results and those of the experiments showed good agreement. Serrette [11] reviewed the European code for lateral buckling (Eurocod 3) and stated that the specifications, design considerations and recommedations provide a consistent and unified method for single, double and nonsymmetric sections. he compared Eurocod 3 To AISC-LRED to show the deficiencies in the latter code.

While the problem of general and local buckling of hollow thin columns been considered by some investigators, the problem of stiffened hollow columns seems to be remained untouched. This is in part due to the uncertainties in distinguishing between long and short columns on one hand, and thin and thick columns on the other [12,13], and in part due to the complexities in exact analysis of the stability problem. However, the analysis may be performed employing the approximate methods of energy such as the Ritz method. This method is used in the present paper to analyze sleeve-stiffened hollow columns. The columns are assumed to be long and slender, so that general Euler buckling mode prevails over local shell buckling [12]. Both rounded and box section columns are considered in the analysis. To use energy methods, it is necessary to assume an approximate deflection curve which must satisfy the essential boundary conditions. For pin ended columns, the appropriate deflection curve takes on the form:

$$y = A\sin\frac{\pi x}{l} \quad \text{(a)}$$

where A is the coefficient to be determined via analysis and/is the length of the column. When the

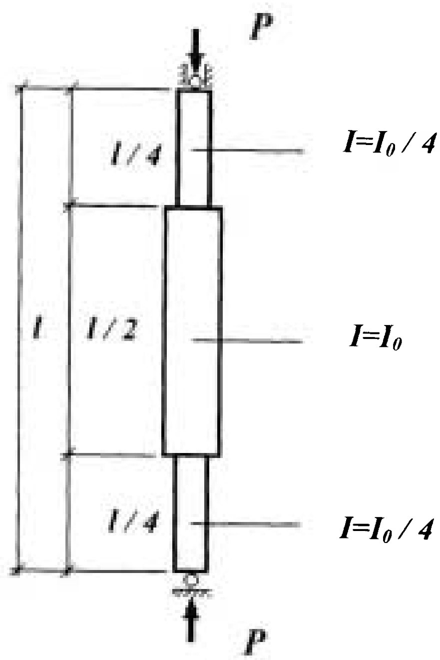

Figure 1. Stepped column with variable moment of inertia.

above deflection form is used to find the critical load for a pin-ended stepped solid column, as shown in Figure 1, the results shows an error of 33 percent compared to that of the exact solution [12]. Assuming a two-term delfection curve of the form;

$$y = A\sin\frac{\pi x}{l} + B\sin\frac{3\pi x}{l} \qquad \text{(b)}$$

The error decreases to 13 percent [12]. However, for a three-term deflection curve, as:

$$y = A\sin\frac{\pi x}{l} + B\sin\frac{3\pi x}{l} + C\sin\frac{5\pi x}{l} \qquad \text{(c)}$$

the algebra involved is so lengthy and tedious to perform that manual computation seems indomitable and has not been attempted in the classical works. With the development of powerful software packages like "MATHEMATICA", it is now possible to approach such problems. Actually this latter form for the deflection function was assumed by the authors of the present paper to find that the error reduces to 2.5 percent for the above-mentioned column. Nevertheless it should be noted that even using "MATHEMATICA", the computations take a relatively long time on the computer and the end results are so lengthy that occupy several monitor screens.

Hollow columns are favorable in structures over solid columns of the same bending stiffness because not only the columns themselves are made lighter but also the overall weight of the structure is reduced. This is a two-fold material saving. For the compression members in machines, a three-fold saving will be made as the lighter the machine, the lower the energy consumption.

STABILITY ANALYSIS

Consider a stepped hollow column of the total length of **L** as depicted in Figure 2. The column (box or tubular) with bending stiffness of EI_1, is stiffened at the mid-length by a sleeve of length /to EI_2 as shown in Figure 2. The column is assumed to be pin-ended with the axial compressive force **P** applied on it. For such a column without any stiffening, the deflection function may be assumed to be of the form $y = C_1 \sin(\pi x/L)$. To account for the mid-length flatness due to the stiffening sleeve, then, two other sinusoidal terms are added to the above mentioned deflection function to yield:

$$y = C_1 \sin\frac{\pi x}{L} + C_2 \sin\frac{3\pi x}{L} + C_3 \sin\frac{5\pi x}{L} \qquad (1)$$

Due to the symmetry, the deflection energy is:

$$U = 2\frac{EI_1}{2}\int_0^{l_1} (y'')^2\,dx + \frac{EI_2}{2}\int_{l_1}^{l_2} (y'')^2\,dx \qquad (2)$$

and the potential energy:

$$V = \frac{-P}{2}\int_0^{L} (y')^2\,dx \qquad (3)$$

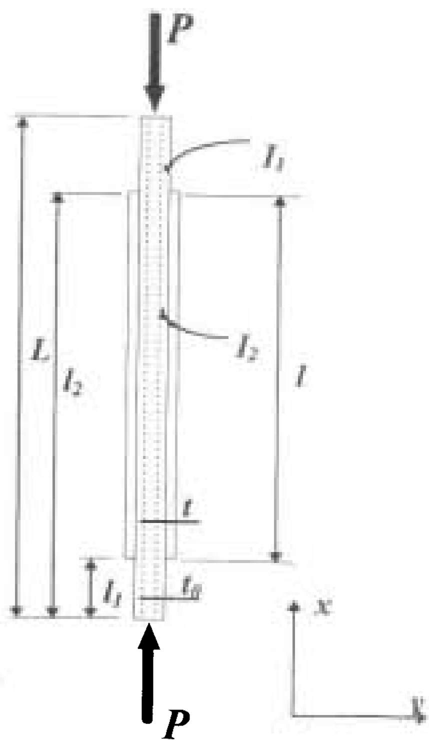

Figure 2. Geometry of the stiffened hollow column.

Differentiating Equation 1 to obtain **y**' and **y**'' and substituting into Equations 2 and 3 yields:

$$
\begin{aligned}
U = {} & \frac{EI_1\pi^3}{L^3}\Big[\frac{c_1^2}{2}\frac{\pi l_1}{L} - \frac{c_1^2}{4}\sin\frac{2\pi l_1}{L} + \frac{81\,c_2^2}{2}\frac{\pi l_1}{L} - \\
& \frac{27\,c_2^2}{4}\sin\frac{6\pi l_1}{L} + \frac{625\,c_3^2}{2}\frac{\pi l_1}{L} - \frac{125\,c_3^2}{4}\sin\frac{10\pi l_1}{L}\Big] + \\
& \frac{EI_2\pi^3}{L^3}\Big[\frac{c_1^2}{2}\frac{\pi(l_2-l_1)}{L} - \frac{c_1^2}{4}\sin\frac{2\pi(l_2-l_1)}{L} + \frac{81\,c_2^2}{2}\frac{\pi(l_2-l_1)}{L} - \\
& \frac{27\,c_2^2}{4}\sin\frac{6\pi(l_2-l_1)}{L} + \frac{625\,c_3^2}{2}\frac{\pi(l_2-l_1)}{L} - \frac{125\,c_3^2}{4}\times \\
& \sin\frac{10\pi(l_2-l_1)}{L}\Big] - \frac{18EI_2c_1c_2L}{\pi}\Big[\sin(\frac{l_1}{L}\pi)\cos(\frac{l_1}{L}\pi)^3 - \\
& \sin(\frac{l_1}{L}\pi)\cos(\frac{l_1}{L}\pi) - \sin(\frac{l_2}{L}\pi)\cos(\frac{l_2}{L}\pi)^3 + \\
& \sin(\frac{l_2}{L}\pi)\cos(\frac{l_2}{L}\pi)\Big] + \frac{EI_2}{2}\Big\{\frac{200L\,c_1c_3}{3\pi}\sin(\frac{l_1}{L}\pi)\times \\
& \cos(\frac{l_1}{L}\pi)^5 + \Big[-\frac{200L\,c_1c_3}{3\pi}\sin(\frac{l_1}{L}\pi)^3 - \frac{625L\,c_1c_3}{6\pi}\times \\
& \sin(\frac{l_1}{L}\pi)\Big]\cos(\frac{l_2}{L}\pi) - \frac{200L\,c_1c_3}{3\pi}\sin(\frac{l_2}{L}\pi)\cos(\frac{l_2}{L}\pi)^5 + \\
& \Big[\frac{200L\,c_1c_3}{3\pi}\sin(\frac{l_2}{L}\pi)^3 + \frac{625L\,c_1c_3}{6\pi}\sin(\frac{l_2}{L}\pi)\Big]\times \\
& \cos(\frac{l_2}{L}\pi)\Big]\Big\} + \frac{112.5EI_2Lc_2c_3}{2\pi}\Big[16\sin(\frac{l_1}{L}\pi)\cos(\frac{l_1}{L}\pi)^7 - \\
& 8\times\sin(\frac{l_1}{L}\pi) + (2\sin(\frac{l_1}{L}\pi)^2+3)\cos(\frac{l_1}{L}\pi)^5 + \sin(\frac{l_1}{L}\pi)\times \\
& (8\times\sin(\frac{l_1}{L}\pi)^2 + 11)\cos(\frac{l_1}{L}\pi)^3 - \sin(\frac{l_1}{L}\pi)(\sin(\frac{l_1}{L}\pi)^2 + \\
& 3)\times\cos(\frac{l_1}{L}\pi) - 16\sin(\frac{l_2}{L}\pi)\cos(\frac{l_2}{L}\pi)^7 + 8\sin(\frac{l_2}{L}\pi) \\
& \times(2\sin(\frac{l_2}{L}\pi)^2+3)\cos(\frac{l_2}{L}\pi)^5 - \sin(\frac{l_2}{L}\pi)(8\sin(\frac{l_2}{L}\pi)^2 + \\
& 11)\times\cos(\frac{l_2}{L}\pi)^3 + \sin(\frac{l_2}{L}\pi)(\sin(\frac{l_2}{L}\pi)^2 + 3)\cos(\frac{l_2}{L}\pi)\Big]
\end{aligned}
\tag{4}
$$

And:

$$v = -\frac{P\pi^2}{4L}(c_1^2\pi + 9c_2^2\pi + 25c_3^2\pi) \tag{5}$$

For the column to take a stable buckled shape, the total energy $(U + V)$ which is a function of the three coefficients $\mathbf{c_1}$, $\mathbf{c_2}$ and $\mathbf{c_3}$ should satisfy the equations:

$$\frac{\partial(U+V)}{\partial c_i} = 0 \quad \text{and} \quad i = 1, 2, 3 \tag{6}$$

Inserting **U** and **V** from Equations 4 and 5 into Equation 6, performing the mathematical operations with the aid of the "MATHEMATICA" software package and simplifying the results, a set of three equations is obtained as:

$$
\begin{aligned}
& c_1(A_1+P.F_1) + c_2A_2 + c_3A_3 = 0 \\
& c_1B_1 + c_2(B_2+P.F_2) + c_3B_3 = 0 \\
& c_1E_1 + c_2E_2 + c_3(E_3+P.F_3) = 0
\end{aligned}
\tag{7}
$$

where:

$$A_1 = \frac{EI_1\pi^3}{L^3}\Big[\frac{\pi l_1}{L} - \frac{1}{2}\sin\frac{2\pi l_1}{L}\Big] + \frac{EI_2\pi^3}{L^3}\Big[\frac{\pi(l_2-l_1)}{L} - \frac{1}{2}\sin\frac{2\pi(l_2-l_1)}{L}\Big]$$

$$A_2 = \frac{18EI_2L}{2\pi}\Big[\sin(\frac{l_1}{L}\pi)\cos(\frac{l_1}{L}\pi)^3 - \sin(\frac{l_1}{L}\pi)\cos(\frac{l_1}{L}\pi) - \sin(\frac{l_2}{L}\pi)\cos(\frac{l_2}{L}\pi)^3 + \sin(\frac{l_2}{L}\pi)\cos(\frac{l_2}{L}\pi)\Big]$$

$$A_3 = \frac{EI_2}{2}\Big[\frac{200L}{3\pi}\sin(\frac{l_1}{L}\pi)\Big]\cos(\frac{l_1}{L}\pi)^5 - \Big(\frac{200L}{3\pi}\sin(\frac{l_2}{L}\pi)^3 + \frac{625L}{6\pi}\sin(\frac{l_1}{L}\pi)\Big)\cos(\frac{l_1}{L}\pi) - \frac{200L}{3\pi}\sin(\frac{l_2}{L}\pi)\Big]\times \cos(\frac{l_2}{L}\pi)^5 + \frac{200L}{3\pi}\sin(\frac{l_2}{L}\pi)^3 + \frac{625L}{6\pi}\sin(\frac{l_2}{L}\pi)\Big)\times \cos(\frac{l_2}{L}\pi)\Big]$$

$$B_1 = \frac{18EI_2L}{2\pi}\Big[\sin(\frac{l_1}{L}\pi)\cos(\frac{l_1}{L}\pi)^3 - \sin(\frac{l_1}{L}\pi)\cos(\frac{l_1}{L}\pi) - \sin(\frac{l_2}{L}\pi)\cos(\frac{l_2}{L}\pi)^3 + \sin(\frac{l_2}{L}\pi)\cos(\frac{l_2}{L}\pi)\Big]$$

$$B_2 = \frac{EI_1\pi^3}{L^3}\Big[81\frac{\pi l_1}{L} - \frac{27}{2}\sin\frac{6\pi l_1}{L}\Big] + \frac{EI_2\pi^3}{L^3}\Big[81\frac{\pi(l_2-l_1)}{L} - \frac{27}{2}\sin\frac{6\pi(l_2-l_1)}{L}\Big]$$

$$B_3 = \frac{112.5EI_2L}{2\pi}\Big[16 + \sin(\frac{l_1}{L}\pi)(8\sin(\frac{l_1}{L}\pi)^2 + 11)\times \cos(\frac{l_1}{L}\pi)^3 - \sin(\frac{l_1}{L}\pi)(\sin(\frac{l_1}{L}\pi)^2+3)\cos(\frac{l_1}{L}\pi) -$$

$$16\sin(\frac{l_2}{L}\pi)\cos(\frac{l_2}{L}\pi)^7+8\sin(\frac{l_2}{L}\pi)(2\sin(\frac{l_2}{L}\pi)^2+3)\cos(\frac{l_2}{L}\pi)^5-\sin(\frac{l_2}{L}\pi)(8\sin(\frac{l_2}{L}\pi)^2+11)\times\cos(\frac{l_2}{L}\pi)^3+\sin(\frac{l_2}{L}\pi)(\sin(\frac{l_2}{L}\pi)^2+3)\cos(\frac{l_2}{L}\pi)]$$

$$E_1=\frac{EI_2}{2}\,[\frac{200L}{3\pi}(\sin(\frac{l_1}{L}\pi)\cos(\frac{l_1}{L}\pi)^5-[\frac{200L}{3\pi}\times(\sin(\frac{l_1}{L}\pi)^3+\frac{625L}{6\pi}\sin(\frac{l_1}{L}\pi)]\cos(\frac{l_1}{L}\pi)-\frac{200L}{3\pi}\times\sin(\frac{l_2}{L}\pi)\cos(\frac{l_2}{L}\pi)^5+[\frac{200L}{3\pi}\sin(\frac{l_2}{L}\pi)^3+\frac{625L}{6\pi}\times\sin(\frac{l_2}{L}\pi)]\times\cos(\frac{l_2}{L}\pi)$$

$$E_2=\frac{112.5EI_2L}{2\pi}[16\sin(\frac{l_1}{L}\pi)\cos(\frac{l_1}{L}\pi)^7-8\sin(\frac{l_1}{L}\pi)+(2\sin(\frac{l_1}{L}\pi)^2+3)\cos(\frac{l_1}{L}\pi)^5+\sin(\frac{l_1}{L}\pi)(8\sin(\frac{l_1}{L}\pi)^2+11)\cos(\frac{l_1}{L}\pi)^3-\sin(\frac{l_1}{L}\pi)(\sin(\frac{l_1}{L}\pi)^2+3)\cos(\frac{l_1}{L}\pi)-16\sin(\frac{l_2}{L}\pi)\cos(\frac{l_2}{L}\pi)^7+8\sin(\frac{l_2}{L}\pi)(2\sin(\frac{l_2}{L}\pi)^2+3)\cos(\frac{l_2}{L}\pi)^5-\sin(\frac{l_2}{L}\pi)(8\sin(\frac{l_2}{L}\pi)^2+11)\times\cos(\frac{l_2}{L}\pi)^3+\sin(\frac{l_2}{L}\pi)(\sin(\frac{l_2}{L}\pi)^2+3)\cos(\frac{l_2}{L}\pi)]$$

$$E_3=\frac{EI_1\pi^3}{L^3}[625\frac{\pi l_1}{L}-\frac{125}{2}\sin\frac{10\pi l_1}{L}]+\frac{EI_2\pi^3}{L^3}\times[\frac{625\pi(l_2-l_1)}{L}-\frac{125}{2}\sin\frac{10\pi(l_2-l_1)}{L}]$$

$$F_1=\frac{-\pi^2}{2L}$$

$$F_2=\frac{-9\pi^2}{2L}$$

$$F_3=\frac{-25\pi^2}{2L} \qquad (8)$$

The solution to Equations 7 results in an eigenvalue problem of the from:

$$\begin{vmatrix} A_1+F_1.P & A_2 & A_3 \\ B_1 & B_2+F_2.P & B_3 \\ E_1 & E_2 & E_3+F_3.P \end{vmatrix}\begin{Bmatrix} c_1 \\ c_2 \\ c_3 \end{Bmatrix}=0 \qquad (9)$$

With the characteristic equation:

$$k_1P^3+k_2P^2+k_3P+k_4=0 \qquad (10)$$

where;

$$k_1=F_1F_2F_3$$
$$k_2=F_1F_2E_3+A_1F_1E_3+B_2F_1F_3$$
$$k_3=A_1F_1E_3+E_3B_2F_1+A_1B_2F_3-E_1F_2A_3-E_2B_3F_1-B_1A_2F_3$$
$$k_4=E_3A_1B_2+A_2B_3E_1+A_3E_2B_1-E_1A_3B_2-E_2B_3A_1-B_1A_2E_3 \qquad (11)$$

The characteristic Equation 10 yields three eigenvalues of which the smallest answer represents the critical load $\mathbf{P}_{cr}$:

$$P_{cr}=-2\sqrt{-s}\cos\theta \qquad (12)$$

where s and θ are defined in terms of $\mathbf{k}_1$ through to $\mathbf{k}_4$ as:

$$s=\frac{k_3}{3k_1}-\frac{k_2}{9k_1}$$
$$\theta=\frac{1}{3}\mathrm{Cos}^{-1}\frac{q}{2\sqrt{-s^3}} \qquad (13)$$

where

$$q=\frac{2k_2^3}{27k_1^3}-\frac{k_2k_3}{3k_1^2}+\frac{k_4}{k_1}$$

Because of the tremendous lengthy algebra involved in evaluating $\mathbf{P}_{cr}$ from Equation 12, all of the mathematical manipulations in Equations 8 to 13 are performed using the "MATHEMATICA" software package. The final result for the critical load **P** is too lengthy to present here, as on the computer's monitor, the answer occupies twenty screens . However, in order to determine the design curves, it just suffices to evaluate the results for $\mathbf{P}_{cr}$ numerically.

NUMERICAL EVALUATION

To pot the design curves, a wide range of hollow columns with round section (pipe) and square section (box) have been considered, as tabulated by Stahl Im Hochbau [14]. For the pipe columns, the diameter "d" ranges from 21.3*mm* up to 558.8*mm* and the thickness "s" of the main body (column without stiffener) ranges from 2*mm* to 8.8*mm*, while the thickness "t " of the sleeve (stiffening portion) varies from 1*mm* to the thickness "s" of the main body in each case. For the box columns; the side "**a**" ranges from 40 *mm* to 260 *mm*, the thickness "s" from 2.9 *mm* to 7.1*mm* and the variable thickness "t" from 1*mm* up to "s" in each case. With these data, Equations 1 through to 13 are solved employing the "MATHEMATICA" package to yield the critical load $\mathbf{P}_{cr}$ for different values of l/L. The results are plotted as design curves in non-dimensional form as typically depicted in Figures 7 to 9 for the pipe (tube) section, and 3 to 6 for the box section. A total of 25 diagrams for the pipe section and 14 diagrams for the box section are prepared in this manner. Each diagram contains 2 to 8 design curves, covering the whole range of the available profiles in "Stahl Im Hochbau". This sums up to 97 design curves for the pipe-columns and 47 for the box-columns.

THE OPTIMAL DESIGN CURVES

Typical design curves are shown in Figures 3 to 9. The dimensions of the main column are presented at the top of each diagram. The abscissa denotes the dimensionless ratio l/L, where L is the length of the main column and l is the length of the stiffening portion (sleeve). This ratio obviously ranges from 0 to 1. The ordinate denotes the dimensionless ratio $\mathbf{P}/\mathbf{P}_{Eu}$, where $\mathbf{P}_{EU}$ is the Euler buckling load for the main column (without the sleeve) and **P** is the critical load for the stiffened column (including the sleeve). The thickness **t** of the sleeve shown on the right side of the diagrams, **t** ranges from 1*mm* to the nearest integer to the thickness of the main column. This means that the thickness of the sleeve does not exceed that of the main column in each case. All of the design curves show a general trend of increasing with the increase in the ratio of l/L. The degree of increase in $\mathbf{P}/\mathbf{P}_{Eu}$ ranges from 6 percent up to 90 percent, depending on the thickness **t** of the sleeve. Comparing the curves in each diagram with each other, two interesting points can be observed. The first point is that for values of $l/L > 0.7$, the increase in $\mathbf{P}/\mathbf{P}_{Eu}$ is negligibly small. In other words, the curves flatten out as the length of the stiffening sleeve, l, approaches 70 percent of the length of the main column L. In terms of material savings, this means that about 15 percent of the material may be saved by limiting the length of the sleeve, without imposing an appreciable decrease in the buckling loud-carrying capacity of the column. This point may also be used in the design of non-stiffened columns, provided that the capacity is checked for yielding too. The second interesting point is that in the useful range of $0 < l/L < 0.7$, as the thickness **t** of the sleeve increases, the slope of the curves increases progressively. This leads to a more beneficial point in material saving as follows. In each diagram containing serveral design curves, for any desired ratio $\mathbf{P}/\mathbf{P}_{Eu}$,it is possible to pinpoint a portion of the curve for which the amount of material used is a minimum. This is carried out by minimizing the volume of the stiffened columns. The optimum portions of the curves are marked on them by bold lines. Considering the design curves for the box and the tube sections, it is observed that for a comparable area-moment of inertial, **I**, the columns with tube sections show a superior increase for $\mathbf{P}/\mathbf{P}_{Eu}$ over box sections. For instance, comparing the design curves for the box sections as in Figure 6 where **I** = 62.7cm^4 with those of pipe sections as shown in Figure 9 with **I** = 79.2cm^4, the maximum increase in $\mathbf{P}/\mathbf{P}_{Eu}$ is about 50 percent versus 90 percent, respectively.

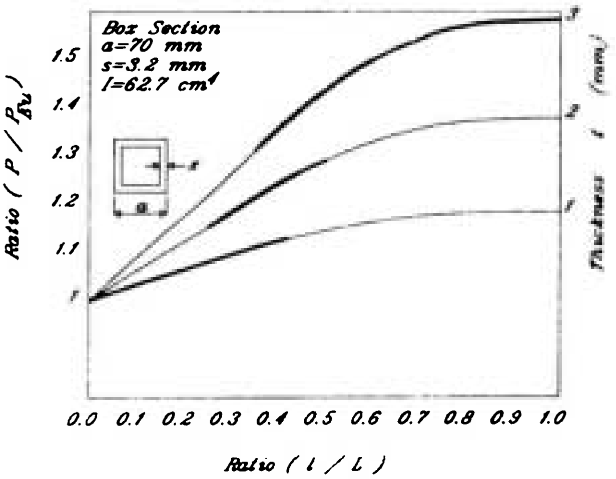

Figure 3. Design curves for box section.

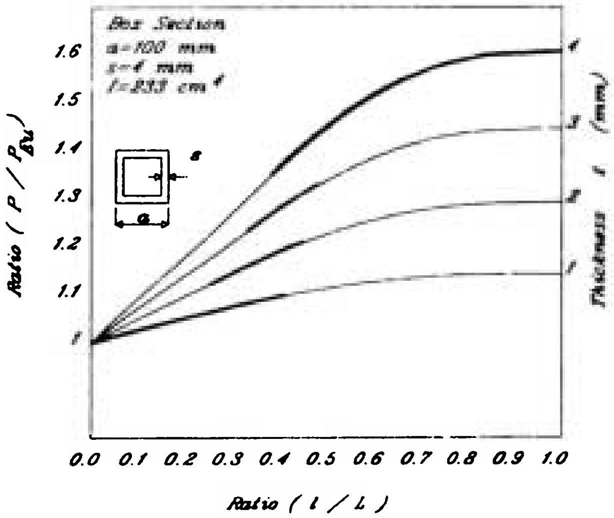

Figure 4. Design curves for box section.

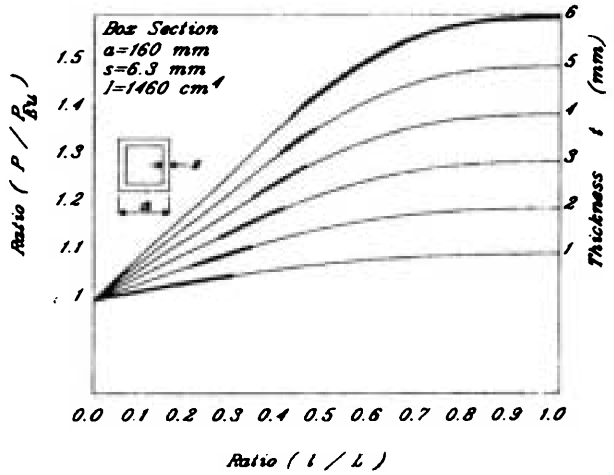

Figure 5. Design curves for box section.

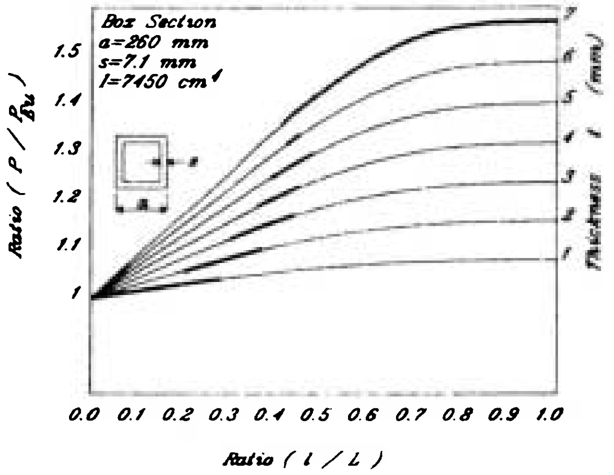

Figure 6. Design curves for box section.

SHELL- BUCKLING CONSIDERATIONS

The stability analysis conducted in this study is based on the Euler-buckling theroy of long and slender columns. Howerver, since the columns are hollow, the analysis should be checked against shell-buckling theory wherever there is an uncertainty about the slenderness of the column to ensure that local buckling does not result in a collapse of the column before the Euler buckling load is reached.

For hollow thin columns, the classical theory of cylindrical shell buckling states thal local buckling

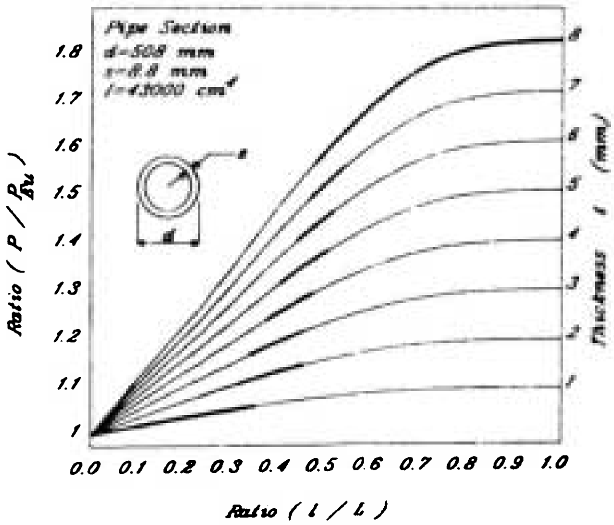

Figure 7. Design curves for pipe section.

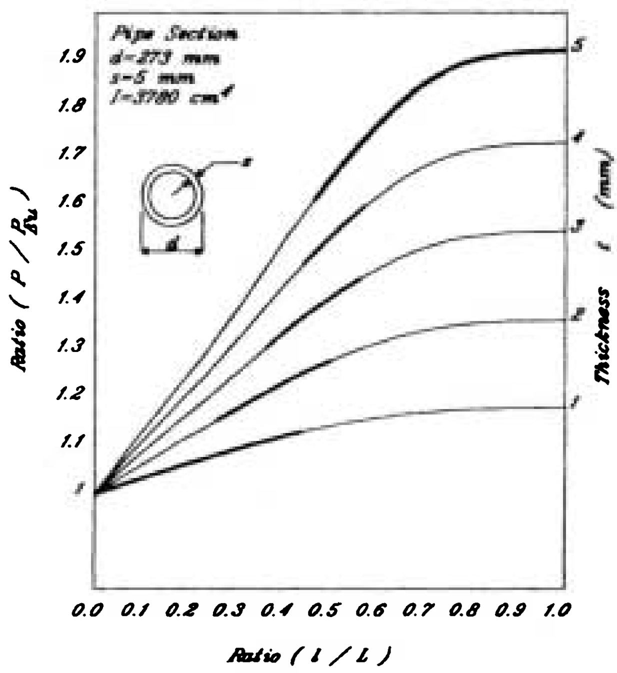

Figure 8. Design curves for pipe section.

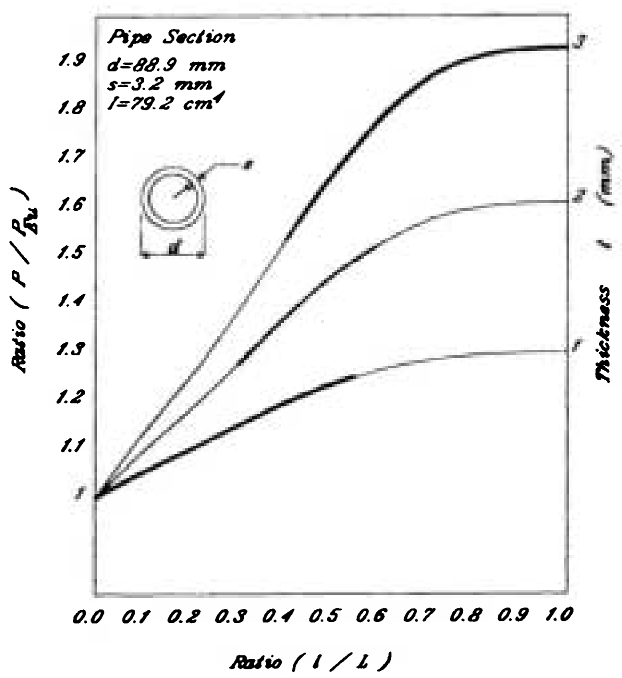

Figure 9. Design curves for pipe section.

may prevail Euler buckling [12]. In order to distinguish between short and long shells, the dimensionless shape factor **z** is defined as [12]:

$$z = \frac{l^2}{rt}(1 - \nu^2)^{1/2} \tag{14}$$

where ν is the poison's ratio and l, **r** and **t** are the length , radius and thickness of the cylindrical shell, respectively. Taking ν as 0.3, Equation 14 takes on the form:

$$z = 0.95\,\frac{l^2}{rt} \tag{15}$$

The critical load $\mathbf{P_{cr}}$ is then determined as:

$$P_{cr} = 0.6\,\frac{EAt}{r} \qquad \text{if} \qquad z > 2.85 \tag{16}$$

$$P_{cr} = \left(1+\frac{12z^2}{\pi^4}\right)\frac{2r\pi^2 A}{tl^2} \qquad \text{if} \qquad z < 2.85 \tag{17}$$

where **A** is the section area, **E** is the Young's modulus and other quantities are as defined beofre.

Equations 16 and 17 are employed to determine the critical load for shell buckling and compared with those of Euler buckling. Precautions are given on the diagrams for the cases where shell buckling may prevail Euler buckling.

For the box-columns, the local plate buckling considerations does not seem necessary, as the thickness of the profiles often inhibits this [5]. From a practical point of view, it is possible to increase the load carring capacity of hollow columns, or equally well to decrease the possibility of local buckling, by filling the column with a cheap material such as compacted soil.

CONCLUSIONS

The stability analysis of sleeve stiffened pin-ended slender hollow columns of pipe or box sections is performed in the present study. This is accomplished using energy method of Ritz, employing three terms in the assumed approximate deflection function, to account for the mid-length flatness due to the stiffening effect of the sleeve. The lengthy and tedious algebraic manipulations involved in computing the resulting integrals and also in solving the relevant eigenvalue problem necessitates employing the powerful and reliable "MATHEMATICA" software. Nevertheless, the final result for the critical load can not be presented in a closed form equation, as it is too long and may occupy several pages. Instead, the "MATHEMATICA" is used again to compute the critical loads numerically for many different box and pipe sizes. In this way, a total of 144 design curves are determined and plotted showing the dimensionless ration $\mathbf{P/P_{Eu}}$ versus l/L for different thicknesses of the stiffening sleeve. The curves show an increasing trend in buckling load-carrying capacity up to 90 perecent. Minimizing the material volume of the sleeves, the optimal portions of the design curves are determined and marked on the curves as bold lines. It is also found that sleeve stiffening beyond 70 percent of the length of the column is a waste of material, as it does not significantly contribute to increasing the load carrying capacity.

For the columns which may not be taken as long and slender, the possibility of local shell buckling is considered. Depending on the shape factor, two different equations are employed to evaluate the critical loads. The results are compared to the critical loads found from the general Euler buckling and precautions are made.

REFERENCES

1. Euler; "De Curvis Elasticis" Additamentum I, Methodus Inveniendi Lineas Curvas Maximi Proprietate Gausdentes, Lausanne and Geneva, (1744).
2. F. R. Shanley, "The Column Paradox", *Journal of the Aeronautical Sciences*, Vol. 13, No. 5, (1946).
3. F. R. Shanley, "Inelastic Column Theory," *Journal of the Aeronautical Sciences*, Vol. 14, No. 5, (1947).
4. N. J. Hoff, "Buckling and Stability," *J. Royal Aeronaut. Soc.*, Vol. 58, Aero Reprint No. 123, (1954).
5. B. G. Johnston, (Ed), "Stability Design Criteria for Metal Structures", 4th ed. New York, Wiley, (1988).
6. W. T. Koiter, I. Elishakoff, Y. W. Li and J. H. Stanres Jr, "Buckling of an Axially Compressed Cylindrical Shell of Variable Thickness", Procedings of the 1993 ASME Winter Annual Meeting, New Orleans, LA, USA, (1993).
7. C.T.F. Ross and M. Humphries, "Buckling of Corrugated Circular Cylinders Under Uniform External Pressure", Thin-walled Struct,. Vol. 17, No. 4. (1993).
8. E. Barbero and J. Tomblin, "Euler Buckling of Thin-walled Composite Columns", Thin-walled Struct., Vol. 17, No. 4, (1993).
9. C. M. Wang, S. Kitipomachai and K. M. Liew, "Research on Elastic Buckling of Columns, Beams and Plates: Focusing on Formulas and Design Charts", *J. Const. Steel Res.*, Vol. 26, No. 2-3, (1993).
10. Y. Lin, N. S. Trahair and S. Rajasekaran, "Energy Equations for Beam Laetral Buckling," Res. Rep., Univ. Sydney; Civ. Min. Eng., No. 635, (1991).
11. R. L. Serrette, "Lateral Buckling; a Comparison of AISC-LRFD and Eurocod3", Proceeding of Structures Congress 1994, Atlanta, GA., USA., Published by ASCE, NY., USA., (1994).
12. A. Chajes, "Principles of Structural Stability", Englewood Cliffs, NJ., Prentice-Hall, (1974).
13. E.P. Popov, "Engineering Mechanics of Solids", Prentice-Hall, (1990).
14. Stahl Im Hochbau, "HandBuch", M.B.H. Verlag Stahleisen, Dusseldorf, (1977).